



Implementing and Characterizing Real-Time Broadband RFI Excision System for the GMRT Wideband Backend

Kaushal D. Buch, Kishor Naik, Swapnil Nalawade, Shruti Bhatporia, Yashwant Gupta & Ajithkumar B.

To cite this article: Kaushal D. Buch, Kishor Naik, Swapnil Nalawade, Shruti Bhatporia, Yashwant Gupta & Ajithkumar B. (2018): Implementing and Characterizing Real-Time Broadband RFI Excision System for the GMRT Wideband Backend, IETE Technical Review, DOI: [10.1080/02564602.2018.1450650](https://doi.org/10.1080/02564602.2018.1450650)

To link to this article: <https://doi.org/10.1080/02564602.2018.1450650>



Published online: 11 Apr 2018.



Submit your article to this journal [↗](#)



View related articles [↗](#)



View Crossmark data [↗](#)



Implementing and Characterizing Real-Time Broadband RFI Excision System for the GMRT Wideband Backend

Kaushal D. Buch, Kishor Naik, Swapnil Nalawade, Shruti Bhatporia, Yashwant Gupta and Ajithkumar B.

Digital Backend Group, Giant Metrewave Radio Telescope, National Centre for Radio Astrophysics – Tata Institute of Fundamental Research, Pune, India

ABSTRACT

The Giant Metrewave Radio Telescope (GMRT) is being upgraded to increase the receiver sensitivity. This makes the receiver more susceptible to man-made Radio Frequency Interference (RFI). To improve the receiver performance in the presence of RFI, real-time RFI excision (filtering) is incorporated in the GMRT wideband backend (GWB). The RFI filtering system is implemented on FPGA (Field Programmable Gate Array) and CPU (Central Processing Unit)–GPU (Graphics Processing Unit) platforms to detect and remove broadband and narrowband RFI, respectively. The RFI is detected using a threshold-based technique where the threshold is computed using Median Absolute Deviation (MAD) estimator. The filtering is carried out by replacing the RFI samples by either noise samples or constant value or threshold. This paper describes the status of the real-time broadband RFI excision system in the wideband receiver chain of the upgraded GMRT. The methodology for carrying out various tests to demonstrate the performance of broadband RFI excision at the system level and on the radio astronomical imaging experiments is also described.

KEYWORDS

GMRT; GWB; Median Absolute Deviation; Radio telescope; RFI; RFI mitigation

1. INTRODUCTION

Giant Metrewave Radio Telescope (GMRT) is an array consisting of 30, 45-m diameter parabolic reflector antennas [1]. It is a passive radiometer for observing astrophysical phenomena occurring in the universe at radio frequencies from 150 to 1450 MHz. As a part of the upgraded GMRT (uGMRT) project, the instantaneous bandwidth of the GMRT receiver is increased from 32 to 400 MHz to improve the sensitivity [2]. As a result, the uGMRT receiver is now susceptible to man-made Radio Frequency Interference (RFI). In order to achieve desired sensitivity in the presence of RFI, an RFI excision system is incorporated in the uGMRT receiver chain. This FPGA (Field Programmable Gate Array)-based RFI excision system operates in real-time for filtering broadband RFI on time-series of individual antennas. It is released as a part of the uGMRT system and is currently undergoing system-level testing for understanding the effects of broadband RFI filtering.

RFI excision techniques use a robust statistical estimator to estimate the dispersion of the signal and the filtering thresholds [3,4]. The signal values outside the threshold are blanked (replaced by zeros) or held at the threshold. Another approach uses non-normality detection to find and remove blocks of data that deviate from the normal distribution due to RFI [5]. The RFI excision technique

used for uGMRT determines the filtering threshold through robust statistical estimate of dispersion using Median Absolute Deviation (MAD). The samples outside this threshold are replaced by a constant value, threshold, or digital noise [6]. Early work in RFI mitigation at the Westerbork Synthesis Radio Telescope describes FPGA implementation of the algorithm and its effects on the cross-correlation power spectrum as described in [7]. The description in [3,7] provides the details of different estimators, their implementation, and tests. To the best of authors' knowledge, there has been no detailed study and a generic method for testing the effects of real-time RFI excision on different measurement parameters of a radio telescope.

This paper describes the broadband RFI excision technique and its implementation and testing on GMRT wideband backend (GWB) [8]. The contributions of this paper are:

- A comparative analysis of the signal with and without real-time broadband RFI filtering for the two different signal processing modes (correlator and beamformer) of the GWB.
- Analysis and results from controlled tests carried out using a programmable analog instrument developed at the GMRT to emulate desired type of RFI signal of a required strength.

- The system performance in the presence of RFI by measuring improvement in the cross-correlation between antenna pairs and assessing the quality of astronomical imaging.

The paper is organized as follows – Section 2 provides details of RFI excision technique, properties of RFI, and the implementation of the RFI filtering system on GWB. Section 3 describes the test setup, system configuration, and results from the various system tests and imaging experiments carried out for the broadband RFI excision. Section 4 provides discussion and future work.

2. REAL-TIME BROADBAND RFI EXCISION IN THE GWB

This section provides an overview of the broadband RFI, its sources around the GMRT and its effects on the astronomical signal. This is followed by a brief introduction to the GWB and the technique used for broadband RFI mitigation in the uGMRT.

2.1 Broadband RFI at the GMRT

Broadband RFI is a result of impulsive events in time-domain which leads to an increase in the power across the spectrum. At the GMRT, the sources of broadband RFI are sparking (gap discharge) on high-voltage lines or transformers, corona discharge, and vehicular sparking in the vicinity of the telescope. RFI caused due to sparking on high-voltage AC transmission lines is periodic over multiples of line frequency (50 Hz in India) – 10 ms for a single-phase line and 3.3 ms for a three-phase line. This type of RFI is observed as a group of strong impulses, 10–20 dB higher than the system noise and a duration of few tens of microseconds. Individual impulses generally have duration of tens of nanoseconds. The severity and strength of broadband RFI observed at the GMRT is stronger at lower radio frequencies and worsens during pre-monsoon and monsoon season. Strong broadband RFI superimposes on the Gaussian distributed astronomical signal and makes the distribution of the resulting signal otherwise wide-sense stationary, heavy-tailed [3].

2.1.1 Effects of Broadband RFI

Broadband RFI introduces a non-random component to the astronomical signal. As a result, the fluctuations in the measurement do not reduce upon temporal integration as per the radiometer equation, i.e. \sqrt{BT} where B is the receiver bandwidth in Hertz and T is the integration

time in seconds. The degradation in the signal-to-noise ratio (SNR) due to broadband RFI limits the detection of weak radio astronomical sources. Real-time RFI excision reduces the effects of broadband RFI significantly by removing it at an early stage (pre-detection or pre-correlation) in the signal processing chain.

2.2 GWB

GWB is a real-time signal processing system for the uGMRT receiver [8]. It is implemented using a combination of FPGAs and GPUs (Graphics Processing Units). This system digitizes the 60 baseband signal inputs (30 antennas with dual polarization) each having an instantaneous bandwidth of 400 MHz. Real-time broadband RFI filtering is carried out for every input at the Nyquist rate (800 MHz) on FPGAs. The digitized time-domain signal is then fed to a compute cluster which consists of high-end CPUs (Central Processing Units) and GPUs. In the current GWB configuration, each FPGA-based hardware board can process up to a maximum of four inputs. GWB performs two main operations on the GPUs—correlation and beamforming on the GPUs. Both these operations are carried out after the signal is transformed into frequency domain (i.e. after Fourier Transformation). The correlator and beamformer outputs are temporally integrated to improve the SNR. The correlator provides auto and cross-correlation spectrum between every pair of antennas at 671 ms (minimum) time resolution whereas the beamformer provides four either incoherent or phased-array beam spectrum at 80 μ s (minimum) time resolution.

2.3 RFI Excision Technique

Broadband real-time RFI excision process in the GWB is split into three parts – robust threshold computation, detection, and filtering. MAD (D) is used for robust estimation of dispersion of the data in the presence of RFI (outliers). D is then scaled to equivalent robust standard deviation (1.4826 times D in case of normal distribution) for determining the upper and lower detection thresholds (τ_U and τ_L)

$$\begin{aligned}\tau_U &= M + n \times (1.4826 \times D) \\ \tau_L &= M - n \times (1.4826 \times D),\end{aligned}\tag{1}$$

around the median M of the data window. The value n decides the multiple of standard deviation that the threshold would be from the median of the data. Each input sample (x_i) in the data window is then compared

with the detection thresholds. The output sample z_i is unchanged if the input sample is within the thresholds

$$\begin{aligned} z_i &= K; & \text{for } x_i \geq \tau_U \text{ or } x_i \leq \tau_L \\ z_i &= x_i; & \text{for } \tau_L < x_i < \tau_U \end{aligned} \quad (2)$$

whereas the samples outside the thresholds are replaced with constant value, threshold, or digital noise [9] (K). MAD estimator is robust up to 50% RFI in a given data window. Thus, the typical duration of RFI and the rate at which the signal is sampled determine the size of the data window for MAD estimation. Since real-time MAD computation over large window sizes is impractical to develop due to hardware resource constraints, an alternate technique called Median of MAD (MoM) [6] is introduced. Instead of depending on one window for estimating the MAD value, MoM (M_D) uses median (M) of the k MAD values

$$M_D = M(D_1, D_2, D_3, \dots, D_k) \quad (3)$$

where $D_1, D_2, D_3, \dots, D_k$ are the MAD values for k successive data windows. MoM-based threshold estimation is useful in mitigating longer bursts of strong RFI.

Currently, the real-time broadband RFI excision system in the GWB has two variants, MAD and MoM. MAD estimation is carried out on a window of 16,384 samples and MoM is a median of 4096 MAD values where each MAD value is estimated over 4096 data samples. For a 1.25 ns sampling period in the GWB, the maximum duration of RFI that the RFI excision system can filter is 40 μ s for MAD and 40 ms for MoM.

3. TESTING BROADBAND RFI EXCISION ON GWB: SCHEMES AND RESULTS

The radio frequency signal is received, processed, and conditioned before digitization as shown in Figure 1. The digitized signal is sent to the FPGA boards where the broadband RFI excision is implemented in time domain. The output of the FPGA boards is fed to a CPU-GPU cluster for correlation and beamforming

operations. The output of this cluster is sent to data acquisition computers for recording the data. Analysis of real-time RFI excision is carried out on recorded data. To observe and analyze the RFI instances before and after RFI filtering, the beamformer output is preferred because of its relatively short integration time. The beamformer mode eases the process of locating the occurrences of broadband RFI in a long stretch of data. Since this technique is implemented for the correlator mode of the GWB, the effect of filtering is checked on the correlator output as well. During some comparison tests, both correlator and beamformer outputs are simultaneously recorded. The results described in this paper are for 2048 spectral channels and an integration time of 1.3 ms (beamformer mode) and 671 ms (correlator mode). The temporal behavior of a single spectral channel is shown in all the results described in this paper. The time axis in all the plots represents the actual Indian Standard Time (IST) of the observations.

3.1 Test Schemes

Broadband RFI filtering is implemented on FPGA board with four digital inputs. The tests were carried out in two different ways using the digital copy of the signals inside the FPGA. The comparison tests are carried out between the same polarizations of different antennas (if not mentioned specifically). An appropriate delay correction has been used in the correlator and beamformer modes to ensure a fair comparison between the unfiltered and filtered data.

- The first option uses the unfiltered and filtered copies of two antennas to be sent to the digital signal processing subsystem for further processing. With this arrangement, the beamformer and correlator outputs can be recorded simultaneously.
- The second option uses a single antenna input copied to all the four inputs out of which three are filtered. This arrangement facilitates simultaneous analysis of two variable parameters of this

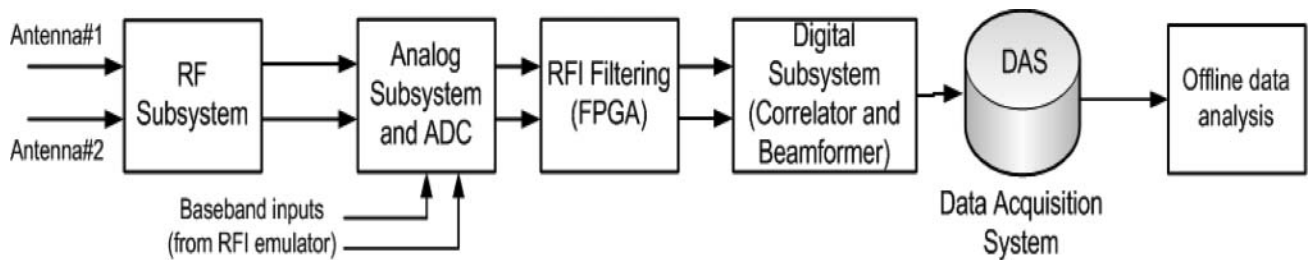


Figure 1: Block diagram of the real-time RFI excision test setup for the uGMRT

filter-threshold value (n) and replacement option (K) for the same antenna input signal.

Quantitative improvement in the SNR was carried out using the metric shown in [4]. The improvement (dB) is given as $10 \log_{10}(S_F/S_U)$ where S_F and S_U are the average mean-to-root mean square (RMS) ratios of the filtered and unfiltered signals, respectively

3.2 Test Results

This section describes the test results from the simultaneous comparison tests between – correlator and beamformer outputs, different replacement options, and MAD and MoM techniques. The replacement options are zero (rp10), threshold (rpbt), and digital noise (rpbdn). This is followed by the test results from the system-level off-source tests and imaging tests.

3.2.1 Simultaneous Comparison Between the Correlator and Beamformer Outputs

The effect of RFI filtering using MAD at 3σ threshold and replacement by zero value for a single GMRT antenna (number C05) can be seen in the subplot (a) of Figure 2. The filtered (blue) and unfiltered (red) outputs are shown in subplot (a) and the corresponding improvement metric in dB is shown in subplot (b). Simultaneous recording in the correlator mode is carried out for colocated antennas in order to observe correlated RFI. It can be seen that the cross-correlation between the unfiltered signals shows an increase in the

power level during instances of RFI (subplot (c)). This increase is brought down as can be seen in the correlation between the filtered signals. A comparison shows that the filtering is stronger for replacement by zero than by a non-zero threshold as seen in subplot (d). Subplot (e) shows the behavior of the phase of the cross-correlation for the unfiltered and filtered options. In subplot (e), the replacement by threshold maintains the phase of cross-correlation constant and hence is better than replacement by zeros where phase changes are observed.

3.2.2 Comparison Between Replacement Options for the Beamformer Output

A simultaneous comparison of the three replacement options (zero, digital noise, and threshold) is carried out on four simultaneous beamformer outputs (as described in Section 3.1). Filtering at 3σ threshold is carried out using MAD technique for GMRT antenna (number C00). The comparison is shown in Figure 3. Subplot (a) shows comparison between unfiltered data (red) and replacement by zero (black). The subplots (b) and (c) show a comparison between unfiltered data (red) and replacement by threshold (green) and digital noise (blue), respectively. Subplot (d) shows the improvement metric for the three replacement schemes. Replacement by zero provides the best improvement as the RFI instances are replaced by a lower value. Replacement by digital noise provides improvement similar to that of replacement by zeros. Replacement by threshold does not provide good improvement as the RFI values are

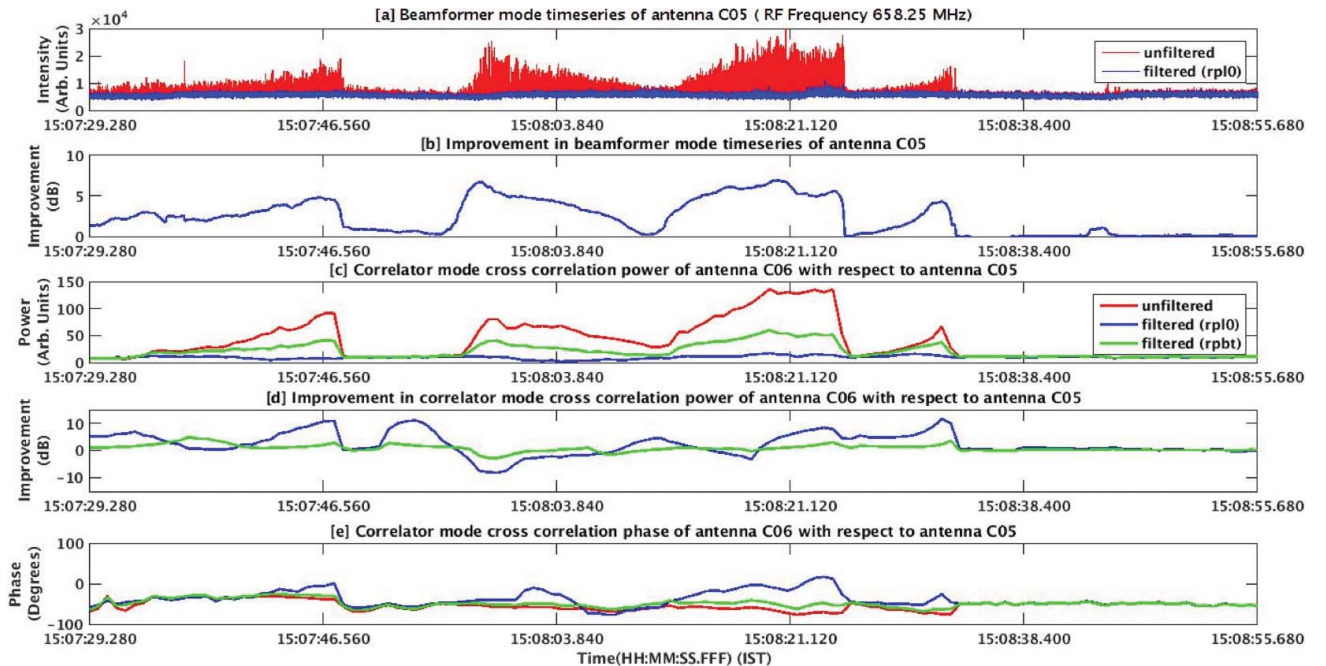


Figure 2: Beamformer and correlator outputs for the comparison between different replacement options

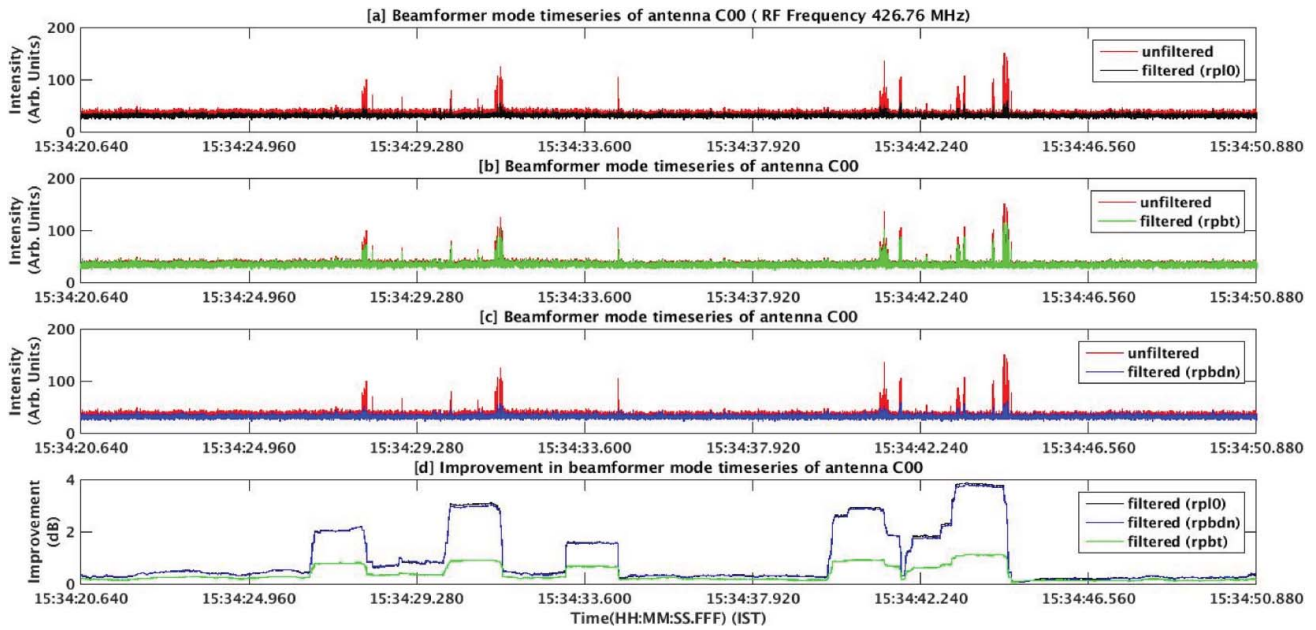


Figure 3: Beamformer outputs for the comparison between different replacements options using the digital copy mode

clipped at the thresholds which are constant higher values as compared to the other two replacement options.

3.2.3 Comparison Between MAD and MoM

A comparison between the MAD and MoM techniques is required to demonstrate their performances under different RFI conditions. The filtering threshold is 3σ . The test setup is similar to that described in Section 3.1. The test is carried out for signal from GMRT antenna (number C09). In Figure 4, subplot (a) shows an overlay of unfiltered (red) and filtered (MAD) (green) technique.

Subplot (b) shows that MoM (blue) performs better over the MAD option. Subplot (c) is the improvement metric for both these techniques. It can be seen, in this particular case, that both the techniques perform well except for one instance where the RFI is excised more strongly using the MoM technique.

A better comparison can be seen in Figure 5 where the same test setup is provided with analog inputs at base-band frequency (Figure 1) through RFI emulator. RFI emulator is an analog instrument developed at the

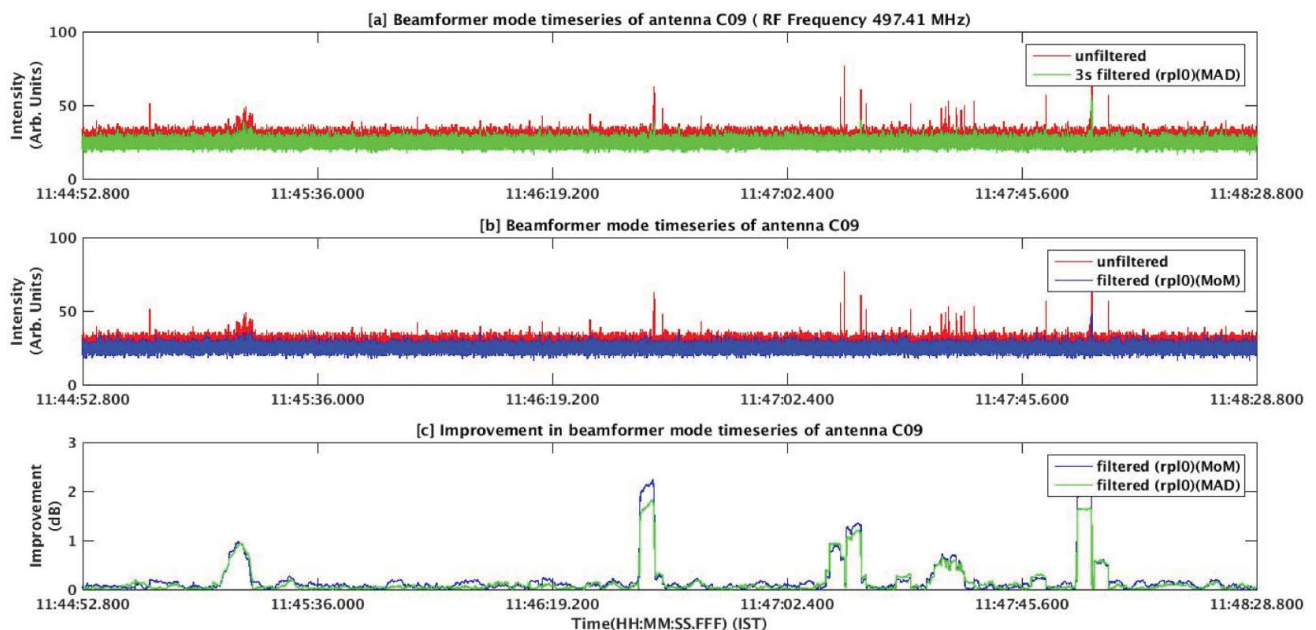


Figure 4: Beamformer outputs from simultaneous comparison between MAD and MoM techniques

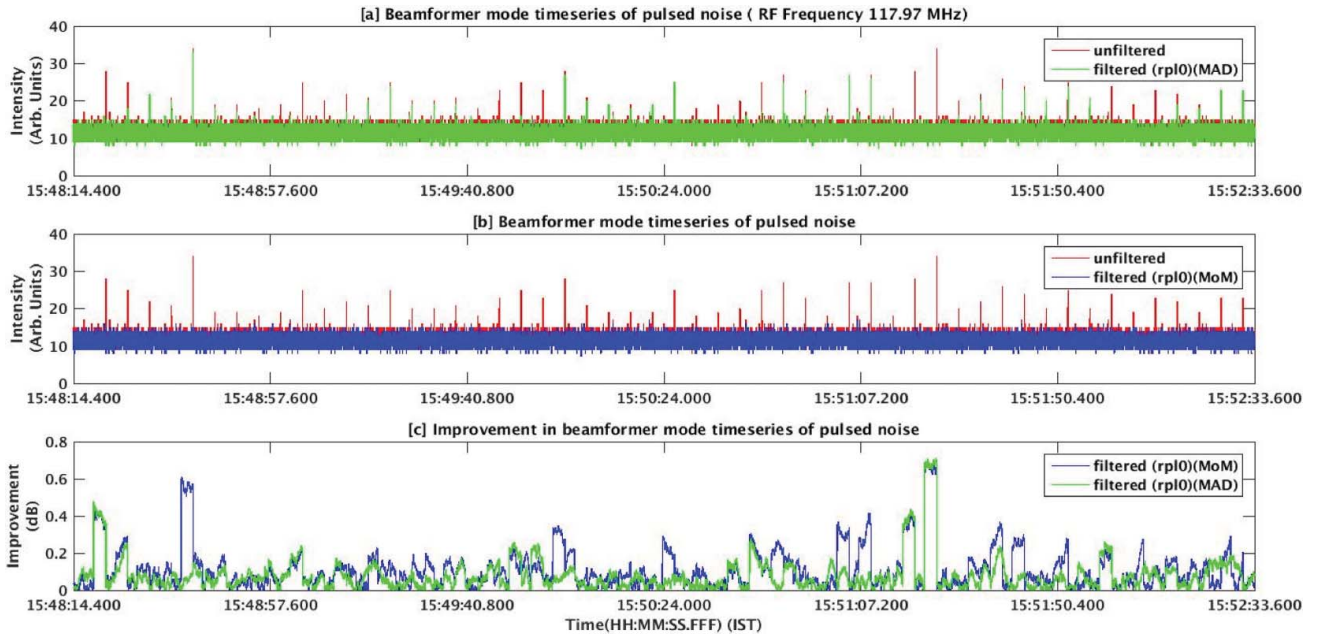


Figure 5: Beamformer outputs from simultaneous comparison between MAD and MoM techniques for emulated RFI signal

GMRT for emulating the behavior of different types of RFI, particularly the broadband RFI from the power-line which has a specific duty cycle [4]. Broadband RFI behavior is emulated with an on-period of 64 μ s and total period of 2 s. It can be seen from Figure 5 that the MAD technique is unable to detect many RFI instances (subplot (a)) particularly those which persist for duration greater than 10 μ s. On the other hand, the MoM technique detects all the RFI instances (subplot (b)). The improvement metric also shows better performance of MoM over MAD (subplot (c)).

3.2.4 Off-Source Tests

Since broadband RFI primarily occurs due to sparking on high-voltage transmission lines around the GMRT array, it is found to be correlated for the closely spaced antennas. As the spacing between the antennas increases, RFI becomes less correlated. This leads to a spurious increase in the correlation even when the antennas are not observing a radio source (i.e. off-source). In order to study the effect of real-time broadband RFI filtering, tests were carried out with the antennas pointing 5 degrees away from the source. Figure 6 shows single spectral channel magnitude and phase of the cross correlation for two short spacing antennas C05-C06 and C06-C13 (left) and two long spacing antennas E03-C06 and W02-C06 (right). Simultaneous observations were carried out to observe the effects with and without filtering in the 250–500 MHz band of uGMRT. For the nearby antenna pairs, the effect of filtering on the magnitude of cross-correlation (subplots

(a) and (c) in the left panel) is significant at 2σ threshold. The post-filtering phase of the correlation (subplots (b) and (d) in the left panel) becomes random indicating the reduction in the correlated component of the filtered signal. The antenna pairs separated by longer distances are not affected as seen in the subplots (e)–(h) in the right panel.

3.2.5 uGMRT Test Observations

A radio image generated from the uGMRT observation is shown in Figure 7. This experimental test setup consisted of 16 antennas having 200 MHz bandwidth in the 250–500 MHz RF band. One of the polarizations (left-circular) is processed through the RFI filter (left image) and the other polarization (right-circular) is processed without the filter (right image). The assumption is that broadband RFI is unpolarized. Power equalization has been ensured between the polarizations. The filtering is carried out at 3σ threshold and the RFI is blanked (replaced by zeros). The image formed without the filter has artifacts and also has a lesser contrast. This is expected as broadband RFI adds to the overall noise floor and hence results in reduced dynamic range of the radio image. It can be seen that the image obtained after RFI filtering is much cleaner and has improved contrast over the one without the filter. In this clean image, it is possible to distinguish a few background radio sources which were obscured due to the effects of RFI in the image without RFI filtering. There is an overall improvement in the noise (RMS value) by a factor of two after RFI filtering for the image shown in Figure 7.

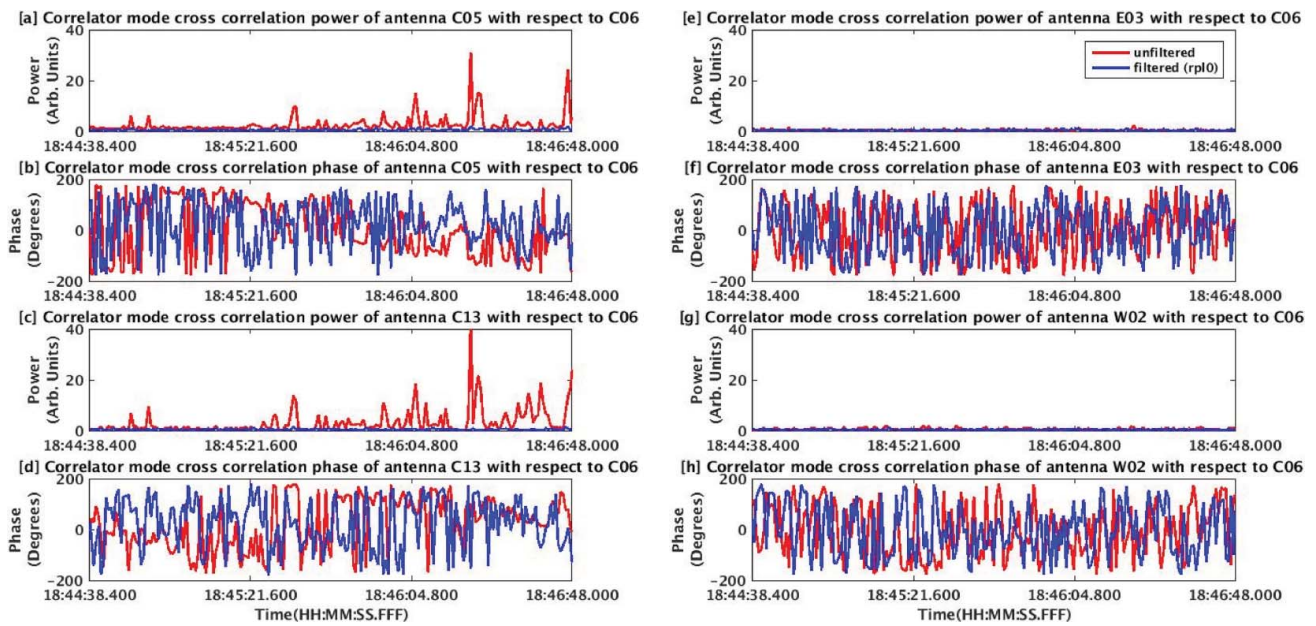


Figure 6: Results from the off-source tests

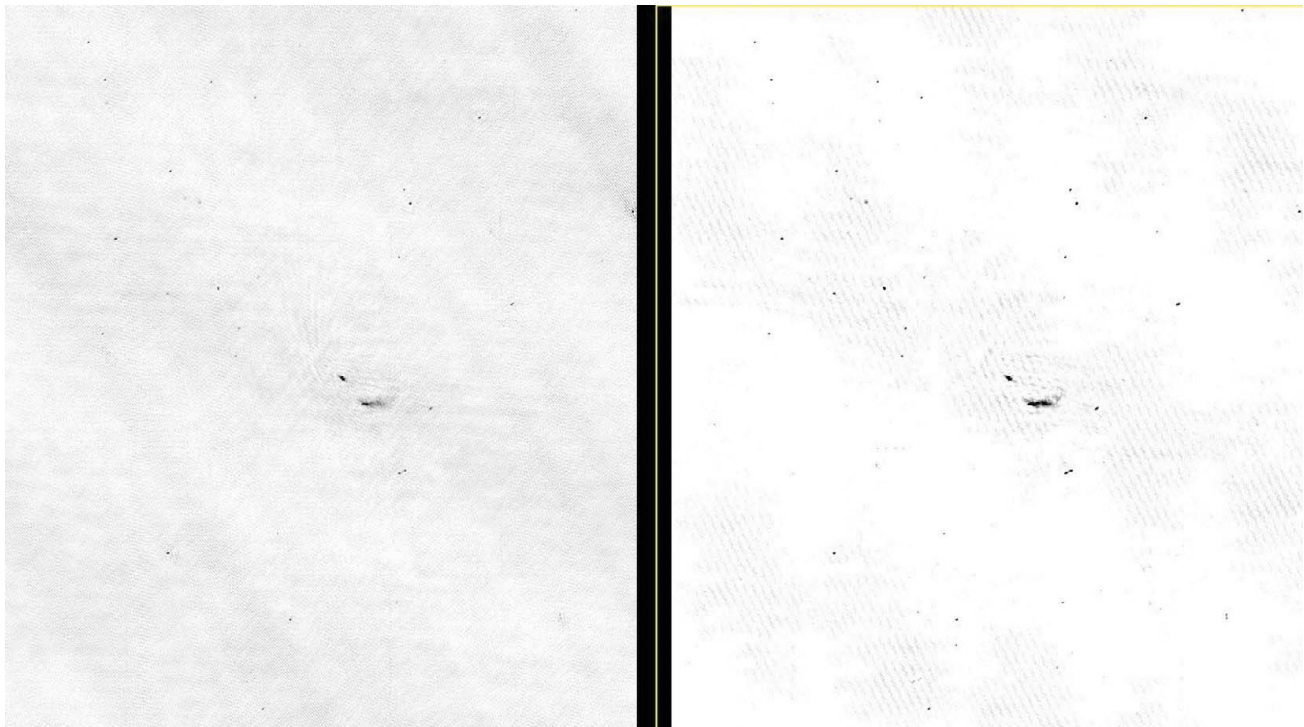


Figure 7: Radio image from 16-antenna uGMRT observation in the 250–500 MHz band with one polarization filtered using the real-time broadband RFI filtering (right) and the other polarization without filtering (left) (Image Courtesy: Dharam Vir Lal)

The diagonal stripes in this image are because of bad baselines which could be due to the presence of correlated RFI. It is seen in both the cases (filtered and unfiltered). This may be due to the presence of strong narrowband RFI (which this filter is not intended to remove) or low-level broadband RFI.

4. DISCUSSION AND FUTURE WORK

The paper described implementation and testing of a real-time broadband RFI excision technique for the uGMRT. Real-time implementations of different variants of this technique which are released for the uGMRT system were

described. The procedure and performance of various methods developed for testing the excision using antenna and emulator signals was described. The results show that the filter is able to significantly reduce the effects of broadband RFI, leading to improved receiver sensitivity. Real-time RFI excision enables better imaging of weak astronomical sources in the presence of strong RFI.

Using the test techniques suggested in this paper, a more detailed analysis of the effects of threshold and replacement options on the various observation parameters and astronomical imaging is being carried out. The techniques described here are generic and can be applied to any radio telescope or radiometer for testing and characterizing real-time RFI excision.

ACKNOWLEDGEMENTS

The authors would like to thank the members of the Backend group and Operations group at the GMRT for their help and support. The authors would also like to thank Dr Dharam Vir Lal and Sanjay Kudale of NCRA-TIFR for their help in planning the test observations, data analysis, and imaging.

DISCLOSURE STATEMENT

No potential conflict of interest was reported by the authors.

REFERENCES

1. G. Swarup, S. Ananthkrishnan, V. Kapahi, A. Rao, C. Subrahmanya, and V. Kulkarni, "The giant metrewave radio telescope," *Curr. Sci.*, Vol. 60, no. 2, pp. 376–80, [Jan. 1991](#).
2. Y. Gupta, B. Ajithkumar, H. Kale, S. Nayak, S. Sabhapathy, S. Sureshkumar, J. Chengalur, R. Swami, S. Ghosh, H. C. Ishwara Chandra, B. Joshi, N. Kanekar, D. Lal, and S. Roy, "The upgraded GMRT: Opening new windows on the radio universe," *Curr. Sci.*, Vol. 113, no. 4, pp. 707–14, [Aug. 2017](#).
3. P. Fridman, "Statistically stable estimates of variance in radioastronomy observations as tools for radio frequency interference mitigation," *Astron. J.*, Vol. 135, no. 5, pp. 1810–24, [May 2008](#).
4. K. Buch, S. Bhatporia, Y. Gupta, S. Nalawade, A. Chowdhury, K. Naik, K. Aggarwal, and B. Ajithkumar, "Towards real-time impulsive RFI mitigation for radio telescopes," *J. Astron. Instrum.*, Vol. 5, pp. 1641018–1–1641018-14, [Jan. 2017](#).
5. RA Series, "Techniques for mitigation of radio frequency interference in radio astronomy," Rep. ITU-R RA.2126-1, [Sep. 2013](#).
6. K. Buch, Y. Gupta, S. Bhatporia, S. Nalawade, K. Naik, and Ajithkumar B., "Real-time RFI excision for the GMRT wideband correlator," in *Proceedings of the 2016 RFI Conference*, Socorro, NM, USA, [2016](#), pp. 11–5.
7. P. Fridman, W. Baan, and R. Millenaar, "Radio frequency interference mitigation at the westerbork synthesis radio telescope: Algorithms, test observations and system implementation," *Astron. J.*, Vol. 128, no. 2, pp. 933–49, [Apr. 2004](#).
8. S. H. Reddy, S. Kudale, U. Gokhale, I. Halagalli, N. Raskar, K. De, S. Gnanaraj, B. Ajithkumar, and Y. Gupta, "A wide-band digital back end for upgraded GMRT," *J. Astron. Instrum.*, Vol. 6, no. 1, pp. 1641011-1–1641011-16, [Jan. 2017](#).
9. K. Buch, Y. Gupta, and B. Ajith Kumar, "Variable correlation digital noise source on FPGA: A versatile tool for debugging radio telescope backends," *J. Astron. Instrum.*, Vol. 3, no. 4, pp. 1450007-1–1450007-7, [Nov. 2014](#).

Authors



Kaushal Buch is working as senior engineer in the digital backend group at the Giant Metrewave Radio Telescope (GMRT), NCRA-TIFR, Pune. A post-graduate in Electronics from S.V. National Institute of Technology Surat, his work at GMRT primarily involves signal processing for the wideband receiver chain of the upgraded GMRT (uGMRT). He is currently working on the design and implementation of digital signal processing algorithms for real-time RFI mitigation and deployment in the uGMRT backend system. He is also involved in the understanding of the signal properties of different types of RFI and its effects on the receiver operation and astronomical imaging.

Corresponding author. E-mail: kdbuch@gmrt.ncra.tifr.res.in



Kishor Naik is working as project engineer in the digital backend group at the GMRT, NCRA-TIFR, Pune. He did post-graduation in microwave and optical communication from Delhi Technological University. He is involved in design and implementation of RFI mitigation techniques in GMRT Receiver.

E-mail: kishornaik33@gmail.com



Swapnil Nalawade is currently working as Research Scientist in Industrial & Meteorological Systems Division of Society for Applied Microwave Electronics Engineering & Research, IIT campus, Mumbai. A graduate in Electronics and Telecommunication from the University of Mumbai, he worked with the Digital Backend Group at GMRT on the development and testing of real-time RFI mitigation techniques.

E-mail: swapnil70737@gmail.com



Shruti Bhatporia is currently working as research assistant at Raman Research Institute. She is a post-graduate in Electronics and Communication Engineering from Institute of Technology, Nirma University, Ahmedabad. She has worked with Digital Backend Group at GMRT on development and testing of real-time RFI mitigation techniques.

E-mail: shrutibhatporia@gmail.com



Yashwant Gupta is Senior Professor and Dean GMRT Observatory, National Centre for Radio Astrophysics, TIFR, Pune. A PhD in Electrical Engineering with specialization in Radio Astronomy from the University of California, San Diego, he has carried out extensive research in various areas of Pulsar astronomy and digital signal processing

and instrumentation for the GMRT receiver. He is leading the effort for upgrading the GMRT systems and is also actively involved in the international consortium for designing and building systems for the Square Kilometer Array project.

E-mail: ygupta@ncra.tifr.res.in



Ajithkumar B. is currently leading the team involved in the design and development of the Backend electronics of the upgraded GMRT Receiver. A post-graduate in Communication Engineering from IIT Mumbai, he has vast experience in the design and implementation of analog and digital signal processing systems. He is involved in the GMRT receiver development from the initial stages of the project and also involved in the RFI related work, mainly on monitoring and classification of RFI data and related aspects.

E-mail: ajit@ncra.tifr.res.in